

# Clock and Data Recovery-Free Data Communications Enabled by Multi-core Fiber with Low Thermal Sensitivity of Skew

Ronit S. Sohanpal, *Student Member, IEEE*, Kari A. Clark, *Student Member, IEEE*, Benjamin J. Puttnam, *Member, IEEE*, Yoshinari Awaji, Naoya Wada, Polina Bayvel, *Fellow, IEEE*, and Zhixin Liu, *Senior Member, IEEE*

**Abstract**—Optical switching has the potential to scale the capacity of data center networks (DCN) with a simultaneously reduction in latency and power consumption. One of the main challenges of optically-switched DCNs is the need for fast clock and data recovery (CDR). Because the DCN traffic is dominated by small packets, the CDR locking time is required to be less than one nanosecond for achieving high network throughput. This need for sub-nanosecond CDR locking time has motivated research on optical clock synchronization techniques, which deliver synchronized clock signals through optical fibers such that the CDR modules in each transceiver only need to track the slow change of clock phase, due to change of the time of flight as temperature varies. It is desired to remove the need for clock phase tracking (and thereby the CDR modules) if the temperature-induced clock phase drift can be significantly reduced, which would reduce the power consumption and the cost of transceivers. Previous studies have shown that the temperature-induced skew change between multi-core fiber (MCF) cores can be forty times lower than that of standard single mode fibers. Thus, clock-synchronized transmission maybe possible by using two different MCF cores for clock and data transmission, respectively, enabling the sharing of an optical clock with stable clock phase. To investigate the potential of MCF for CDR-free short-reach communications, we first improve the measurement method of the temperature dependent inter-core skew change by using a modified delay interferometer, achieving a resolution of 3.8 femtoseconds for accurate inter-core skew measurements. Building on the MCF measurement results, we carried out an MCF-based clock-synchronized transmission experiment, demonstrating the feasibility of CDR-free data communications over a temperature range of 43 °C that meets DCN requirements.

**Index Terms**—Data center networks, clock synchronization, Multi-core fiber, Thermal coefficient of delay.

## I. INTRODUCTION

OPTICAL switching has attracted significant attention in recent research on data center networks (DCN) as it promises a viable route for the further scaling of hyper-scale data center networks, keeping pace with the fast growing traffic of intra-data center interconnections [1]. One of the

major obstacles to optical switching is the requirement for sub-nanosecond clock recovery time, needed to achieve >90 % network throughput [2]. To address this challenge, clock synchronized DCNs have emerged as a promising solution. Previous research has demonstrated a <625 ps clock and data recovery (CDR) locking time in a fast optically-switched DCN with the ‘phase caching’ technique, which actively tracks the clock phase drift caused by the change of environmental temperature. This clock phase tracking is necessary because any temperature drift leads to a change of the optical path length within an optical fiber, and therefore a change in the signal time-of-flight, which can be described by the thermal coefficient of delay (TCD), given in the unit of ps/km/°C [3].

For standard single mode fiber (SMF-28), the TCD is around 39 ps/km/°C [3], meaning the clock phase will drift by one symbol period with merely a 0.5°C temperature change for a 2-km link operating at 25.6 Gb/s. Data center thermal guidelines recommend an air temperature range between 18 °C and 27 °C, with a maximum allowable temperature variation of 40 °C [4]. The measured rate of temperature change in a production data center has been shown to be 0.03 °C/s [2]. Temperature variations within a data center can therefore lead to significant clock phase drift within a short period of time using SMF-28, which necessitates the use of CDR for clock phase tracking.

Alternatively, low thermal-sensitivity hollow-core photonic bandgap fiber (HC-PBGF) with less than 2 ps/km/°C TCD has been shown to significantly increase the tolerance to temperature variation, leading to a temperature tolerance range of 4 °C without actively tracking clock phase, promising a potential to reduce transceiver complexity and power consumption associated with the clock phase tracking [5]. Indeed, if the temperature-induced clock phase change can be reduced to close to zero, clock synchronized data communication without CDR may be possible, benefiting intra-data center interconnects. For example, if transceivers connecting to the same switch can share the same clock source disseminated through the fiber, the latency, power consumption and cost can all be reduced [6].

In recent years, multi-core fiber (MCF) is becoming increasingly popular in DCNs due to its compactness, showing multiple cores co-packaged with optical transceivers for short-reach data communications [7], [8]. A major benefit of homogeneous core MCF, as explored in [9], [10], [11], is the low temperature-induced skew between cores. Recently, a

This work is supported under the Engineering and Physical Sciences Research Council grants (EP/R041792/1 and EP/L015455/1), programme grant TRANSNET (EP/R035342/1) and the Royal Society (PIF/R1/180001).

R. Sohanpal, K. A. Clark, P. Bayvel and Z. Liu are with the Department of Electronic and Electrical Engineering, University College London, London, WC1E 7JE, UK. (email: ronit.sohanpal.14@ucl.ac.uk; kari.clark.14@ucl.ac.uk; p.bayvel@ucl.ac.uk; zhixin.liu@ucl.ac.uk)

B. J. Puttnam, Y. Awaji and N. Wada are with the National Institute of Information and Communications Technology (NICT), Tokyo 184-8795, Japan. (email: ben@nict.go.jp; yossy@nict.go.jp; wada@nict.go.jp)

delay value of a factor of 40 lower than that of two equivalent lengths of standard single-mode fiber (SMF-28) was reported using a 50-km MCF over a 24 °C temperature change [9]. This fits well with the need for low temperature-dependent clock phase shift in clock synchronized DCNs. Nevertheless, the inter-core skew for short (few km) MCF has not been shown, which would confirm that the characteristic low inter-core skew is genuine for short fiber lengths, such as those used in a DCN, rather than an averaging effect of a long fiber. Previous skew measurement methods were based on cross-correlation measurements of data transmission delay, which only provide a skew resolution of hundreds of femtoseconds. This is insufficient to measure the inter-core skew for short-length MCFs (e.g. 2-3 km).

This paper presents the measurement of the temperature-induced inter-core skew for different MCF cores and evaluates the impact of the skew change in clock synchronized transmission systems. To differentiate between the temperature-induced change in absolute propagation delay (as described by the TCD in single-core fibers) and the temperature-induced change in delay difference (i.e. skew) between two MCF cores, we introduce the term thermal coefficient of skew (TCS), as detailed in Section II-A. Section II-B shows the proposed method of TCS measurement using a modified delay interferometer, measuring the skew drift between the center and outer cores with temperature. The TCS of a 3-km, 7-core MCF is characterized at a resolution of 3.8 fs. Based on the measurement results, we demonstrate an MCF-based clock synchronized transmission system in section III, where both clock and data signals are transmitted through two cores of the same MCF. The impact of the temperature variation on bit error rate (BER) performance is characterized in a real-time system. The potential application of the techniques described in this paper is discussed in section IV before the conclusion in section V.

## II. INTER-CORE SKEW MEASUREMENT

### A. Thermal Coefficient of Inter-core Skew

To measure the effect of temperature on the inter-core skew, it is necessary to first understand the physical mechanism by which the temperature affects the propagation delay. First, consider the propagation time (the group delay) of an optical signal through an optical fiber:

$$\tau_g = \frac{n_g L}{c} \quad (1)$$

where  $n_g$  is the group refractive index of the core,  $L$  is the length of the fiber and  $c$  is the speed of light. Taking the derivative of the propagation time with respect to temperature and normalizing by the fiber length, one obtains [12]:

$$\frac{1}{L} \frac{d\tau_g}{dT} = \frac{1}{c} \left( \frac{n_g}{L} \frac{dL}{dT} + \frac{dn_g}{dT} \right) \quad (2)$$

The term on the left-hand side is the thermal coefficient of delay (TCD) for a single-core fiber, in ps/km/°C. The TCD describes how the absolute propagation time of a signal through a fiber changes under temperature variation. The first

term on the right-hand side describes the temperature-induced fiber length expansion, which causes an increase of the optical path length. The second term on the right-hand side refers to the temperature-induced refractive index variation, which is an intrinsic property of the core medium. In SMF-28, the TCD is about 39 ps/km/°C, with the contributions from the fiber expansion and refractive index change given as 2 ps/km/°C and 37 ps/km/°C, respectively [3].

For different MCF core pairs, it is necessary to be able to characterize the temperature-induced skew change, in a similar fashion to the TCD parameter for single-core fibers. However the TCD cannot be used to compare the inter-core skew change, as it only describes the change in absolute propagation delay for a single core. For this reason, the term 'thermal coefficient of skew' (TCS) is defined here, as a characteristic of two core pairs within a MCF. Thus the TCS describes how, for a particular length of fiber, the inter-core skew between two MCF cores varies with temperature. The inter-core skew is given by:

$$\tau_g^{skew} = \tau_{g,1} - \tau_{g,2} \quad (3)$$

where  $\tau_{g,1}$  is the propagation delay in core 1, and  $\tau_{g,2}$  is the propagation delay in core 2. Hence, the TCS becomes:

$$\begin{aligned} \frac{1}{L} \frac{d\tau_g^{skew}}{dT} &= \frac{1}{L} \frac{d}{dT} (\tau_{g,1} - \tau_{g,2}) \\ &= \text{TCD}_1 - \text{TCD}_2 \end{aligned} \quad (4)$$

therefore, the TCS can be expressed as the difference between the TCD values of each core. Thus for two similar cores in the same MCF, the TCS value is expected to be much smaller than the TCD value for either core when signals are co-propagated. This non-zero TCS arises from the slight differences between cores during fiber manufacturing.

To measure the TCS values for a MCF, a delay interferometer was constructed, as shown in Fig. 1. Using a CW signal as the input, two MCF cores are used as two arms of the interferometer, leading to an output power corresponding to the interference between the CW signals in both arms. Heating up the MCF changes the inter-core skew, causing a change in the optical path length between both arms and therefore a change in the output power. Linearly heating up the MCF generates sinusoidal interference fringes, with both arms moving in and out of phase as a result of the changing skew. Each fringe transition from minimum to maximum corresponds to an optical path length change of half a wavelength (optical phase change of  $\pi$ ), resulting in a skew measurement resolution of:

$$\Delta\tau_{res} = \frac{n\lambda}{2c} \quad (6)$$

where  $\lambda$  is the wavelength of the CW source and  $n$  is the core refractive index. It is important to note that this measurement procedure measures the change in "phase delay" skew with temperature,  $d\tau^{skew}/dT$ , which is different from the change in "group delay" skew  $d\tau_g^{skew}/dT$ . From equation 1, the difference between the group delay and the phase delay can be expressed by the difference in the group index and

refractive index, which is given by  $n_g - n = -\lambda \frac{dn}{d\lambda}$  [13]. The measured phase delay skew change with temperature in section II-B showed good agreement with the experimentally observed group delay skew change in section III, thus the measured phase delay skew change can be considered as approximately equivalent to the group delay skew change. For a more accurate estimation of the group delay skew change, the group index or chromatic dispersion at different temperatures needs to be characterised, to find the required correction factor for the group delay skew change calculation [14]. However, this is outside the scope of this paper.

For a 1550 nm CW input and a core refractive index of 1.47, the skew resolution is 3.8 fs. The number of fringe transitions can hence be used to calculate the inter-core skew change, and comparison with the corresponding change in temperature allows for calculation of the TCS for each core pair. The femtosecond-scale resolution allows for greater measurement precision compared to previous measurements, which had a resolution of hundreds of femtoseconds, thus allowing for an accurate measurement of TCS in shorter fiber.

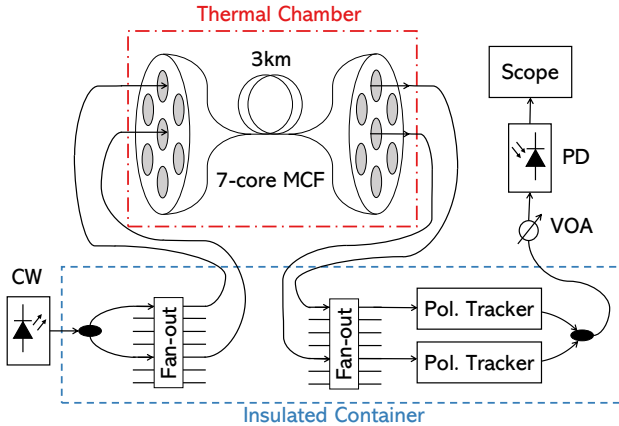


Fig. 1. Delay interferometer setup for the thermal coefficient of skew measurement for 3km 7-core MCF.

### B. TCS Measurement

The CW source used in this experiment was a narrow-linewidth (10 kHz) laser with an output power of 10 dBm at 1550 nm, which was split by a 50:50 polarization-maintaining (PM) coupler. Each arm was connected to two separate cores from a 3-km spool of 7-core MCF via optical fan-outs (with a loss less than 1 dB). Each core had the same refractive index (referred to as homogeneous MCF). The fiber had a cladding diameter of 170  $\mu\text{m}$  and an average core-pitch of 49  $\mu\text{m}$ , with a hexagonal core geometry. The bending radius of the MCF was 15 cm. The measured inter-core crosstalk (including fan-in/fan-out) at 1550 nm between the centre core and each outer core was found to be, on average, less than -60 dB. Using the center core as a reference, the TCS was measured between the center core and the six outer cores. This emulates the inter-core skew that would be experienced in a practical MCF-based clock synchronized DCN, with the clock signal transmitted in the center core and data signals transmitted in the outer cores.

After transmission through the MCF, the two arms were connected to two polarization trackers to align the state of polarization (SoP) to the slow axis of their PM fiber output. This was necessary due to the variation of the output polarization state with temperature across the length of the fiber, since the MCF cores were not PM. This SoP variation lead to a modulation of the detected optical power and thus a periodic reduction of the fringe visibility, which was avoided by tracking and correcting the change in polarization.

The polarization-aligned outputs were combined by a 50:50 PM coupler, and the interfered light was detected by a photodiode and captured by a real-time oscilloscope for data processing. The MCF spool was placed in a thermal chamber, in which the internal temperature was increased approximately linearly from 30  $^{\circ}\text{C}$  to 40  $^{\circ}\text{C}$  at a rate of approximately 0.05  $^{\circ}\text{C}/\text{s}$ . The fan-outs were not placed within the thermal chamber to ensure only the MCF was experiencing heating. Five temperature sensors (resolution 0.05  $^{\circ}\text{C}$ ) were placed at different locations within the thermal chamber to closely monitor the internal temperature, with all five readings averaged for the TCS calculation.

While the skew resolution of the setup is 3.8 fs (using equation 6), in practice the system resolution was limited by the ambient temperature variations in the laboratory, which caused additional skew change during the measurement. To minimize this error, the optical components were sealed within a thermally insulated container, with additional insulating material used to enclose the exposed MCF as it moved between the thermal chamber and insulated container. Thermal gel pads were placed over the optical components to act as thermal heat sinks, reducing the impact of temperature fluctuations in the laboratory.

To quantify the impact of the residual laboratory temperature variation on the system, the thermal chamber and sealed insulated container were left to stabilize over 24 hours, and a subsequent interference fringe measurement was recorded over 8000s. A temperature sensor was placed outside the container to monitor the laboratory temperatures, and the four other sensors were placed within the insulated container. The temperature change over this period within the laboratory and within the insulated container is shown in Fig. 2. The maximum temperature variation within the laboratory was 0.69  $^{\circ}\text{C}$ , and the variation within the insulated container was 0.25  $^{\circ}\text{C}$ , nearly three times lower. The thermal chamber takes approximately 200s to heat across the temperature range of interest (30  $^{\circ}\text{C}$  - 40  $^{\circ}\text{C}$ ), thus the mean ambient skew change within this measurement time represents the error in the TCS measurement. This was found to be 7.1 fs, with a standard deviation of 5.2 fs. This error includes the impact of the temperature change on the SMF patch cords and MCF fan-outs, as well as any additional heat generated by the polarization trackers.

It should be noted that the delay interferometer method was first used to measure the TCD of single-core fibers [3], however using the previously-reported method it was not possible to measure multi-km long fiber due to SoP variations. The addition of polarization tracking, low phase noise CW source and a high thermal stability of the insulated container

allowed for the delay interferometer to be used for km-long fiber skew measurements.

The measured change in inter-core skew against temperature for different core pairs can be seen in Fig. 3. The inter-core skews increase almost linearly with temperature, and any deviations may be attributed to non-uniform heating within the thermal chamber. Note that the delay interferometer method cannot distinguish the skew direction, since it is not possible to identify whether the interference fringes were generated by positively or negatively changing skew. For this reason, Fig. 3 only shows the absolute variation in skew with temperature, and therefore the skew difference between cores cannot be inferred. The sign of the skew gradient can be determined by measuring the change in time-of-flight through two different cores.

The gradient of the skew change in Fig. 3 gives the TCS for that core pair, as shown in Fig. 4. The core labels are shown in the inset. It was found that the worst performing MCF core pair (pair 1-5) had a TCS of 40 fs/km/°C, with an average TCS of 23 fs/km/°C across all measured core pairs. This indicates a strong correlation between MCF cores under temperature variation. This result is also in agreement with previous studies, which have shown dual-core transmission in a MCF to be significantly more temperature insensitive than transmission through two SMF under the same thermal conditions [9] [10].

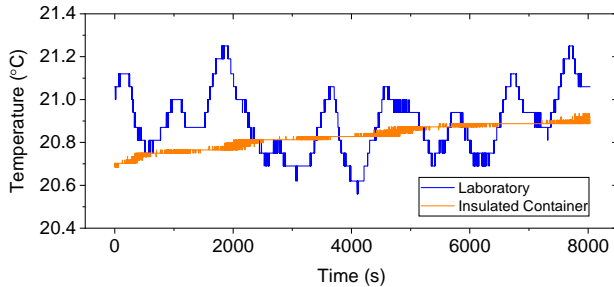


Fig. 2. Change in the laboratory temperature (blue) and insulated container temperature (red) with time during the measurement of the ambient inter-core skew.

### III. CLOCK-SYNCHRONIZED TRANSMISSION

To investigate the application of MCF in optically-switched DCNs, a real-time clock synchronized transmission system was constructed around the MCF, as shown in Fig. 5. Using this setup, a clock and data signal were both sent through the MCF from the transmitter node to the receiver node, with the BER calculated at the receiver node. With the CDR switched off, increasing the temperature of the MCF causes the clock and data signals slowly drift out of phase, resulting in a degradation of the BER. This setup therefore allows experimental evaluation of the impact of the MCF TCS on the BER of a clock synchronized DCN without CDR.

A CW laser with 13 dBm output power at 1550 nm was split by a 50:50 coupler for the optical clock and data modulation. A Mach-Zehnder Modulator (MZM) modulated an 800 MHz reference clock onto one CW arm and was split and sent to two Field Programmable Gate Arrays (FPGAs, Xilinx VCU108),

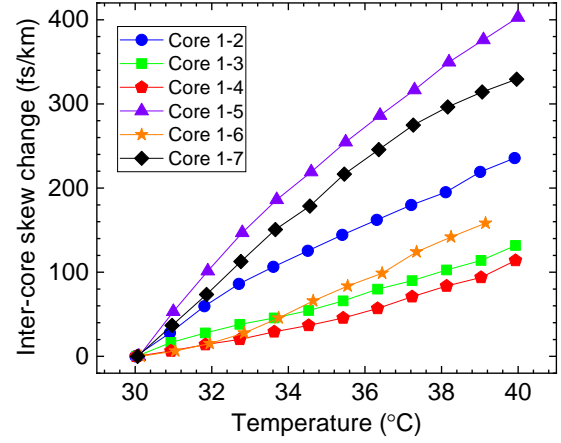


Fig. 3. Change in the measured inter-core skew with temperature between the center core and outer cores. The inter-core skew change has been normalized from 30°C.

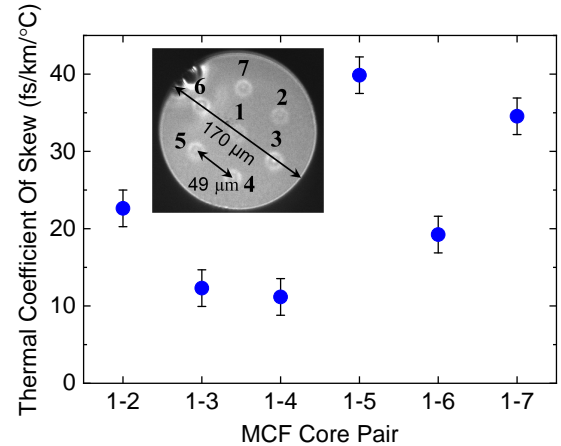


Fig. 4. Comparison of the TCS values for different core pairs. The error is normalized for the fiber length. The inset shows the core profile of the MCF.

which represented the network nodes. The optical clock was sent to the Tx FPGA via a short fiber patch cord. The other branch was connected to the center core of the 3-km 7-core MCF (core 1). 25.6 Gb/s on-off keying (OOK) (PRBS  $2^{31}$ ) was modulated onto the same wavelength via a 30-GHz electro-absorption modulator (EAM), and was sent through one of the outer cores for co-propagating with the clock. Using the same wavelength for clock and data signals allowed for evaluation of the worst-case system performance with the strongest inter-core cross talk [15]. The co-propagation scheme is able to harness the low TCS property of MCF for the clock synchronized DCN, where the clock and data phases drift in the same direction.

After transmission, both the clock and data signals were attenuated down to -10.5 dBm, to remain consistent with data center transmission standards and to emulate optical clock splitting in a cloud DC [16]. The data signal was detected by a 20 GHz receiver before being sent to the Rx FPGA. The 800 MHz optical clock was detected by a 1.2-GHz photodiode and was used as the reference clock of the Rx FPGA. On both FPGAs, the received optical clock signals

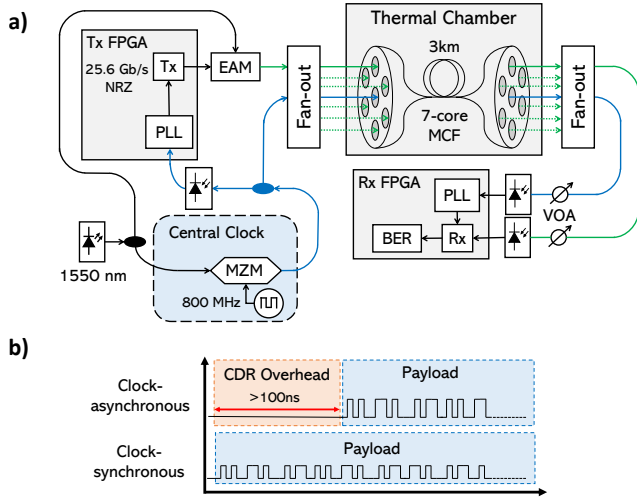


Fig. 5. a) MCF-based clock-synchronized transmission setup. PLL: Phase locked loop. EAM: Electro-absorption modulator. b) Comparison between clock-synchronous and clock-asynchronous transmission latency.

were converted into 800 MHz digital clock signals for clock frequency synchronization, using digital phase-locked loop modules on the FPGAs.

As conceptually shown in Fig. 5b, the synchronized clock allowed for direct detection of the data payload without any extra delay required for CDR (which can be hundreds of nanoseconds [1]), achieving sub-nanosecond CDR as required for optically-switched DCN.

To emulate the temperature change in a DCN, the MCF was placed in the same thermal chamber used for the TCS measurement and heated from 25 °C to 65 °C in 10 °C increments. The temperature values were recorded by five temperature sensors surrounding the fiber spool inside the thermal chamber. The chamber temperature was left to stabilize to within a 0.05 °C variation at each temperature before the BER was measured. The BER was measured in real-time over 60s, which corresponds to a total of  $1.5 \times 10^{12}$  bits for a reliable measurement of BER to  $10^{-9}$ .

Before taking measurements, the clock phase was first calibrated such that the minimum BER was in the center of the temperature measurement range (approx. 45 °C). To do this, the clock and data recovery (CDR) module on the Rx FPGA was turned on and the clock phase for optimum BER was recorded. The experimentally obtained TCS for each core pair was then used to calculate the phase offset required to ensure the optimum BER occurred at 45 °C. The Rx FPGA CDR module was switched off after the initial phase calibration, leaving only the phase lock loop (PLL) with a simple multiplication function to convert the 800 MHz reference clock to 25.6 GHz for data transmission/detection. As the MCF temperature increased, the clock and data phase offset reduced, reducing the BER to optimum at 45 °C. Further increasing the temperature increased the clock phase offset, changing the BER. This usually results in a ‘bathtub’ plot, which allows for evaluation of the temperature range across which the BER can be considered error-free. [5]

It was found that across the entire temperature range of

measurement (40 °C), no bit errors were detected for data transmission through all outer MCF cores. This is in strong agreement with the experimentally obtained TCS values. Assuming the worst case TCS of 40 fs/km/°C, for the 3km MCF and 40 °C temperature range the expected skew change is 4.8 ps, which is only 12% of a symbol period for 25.6 Gb/s OOK.

Using the optically disseminated clock, the Rx FPGA recovered clear opened eye diagrams. Fig. 6 shows the obtained eye diagrams at the receiver power of -10.5 dBm and -16.5 dBm, respectively, both at the same temperature of 22 °C. It was noted that there was no change in the recovered eye diagrams with temperature, as the temperature only affected the clock phase and not the received optical power (eye opening). The white area in the eye diagrams represents the error-free (BER <  $10^{-9}$ ) region. At a received optical power of -10.5 dBm, a clear open eye with an error-free eye width of 19 ps was recorded (48% of a symbol period). Assuming the worst case TCS of 40 fs/km/°C and a 3km MCF, this implies a tolerance to more than 150 °C temperature variation.

To be able to observe the impact of the femtosecond TCS on clock-synchronized systems, the received data signal power was then intentionally attenuated to -16.5 dBm, so that the change in BER due to the temperature-induced clock phase shift could be recorded. The temperature performance of the different MCF cores is shown in Fig 7. For all the measured core pairs, even with a 40 °C temperature variation and 6 dB additional loss, the BER values only changed slightly. It can be seen however that the BER values are not consistent between the core pairs, the discrepancies between cores could be attributed to the slightly different dispersion between the MCF cores and the fan-outs [15].

To evaluate the power penalty caused by the temperature change, the receiver sensitivities for the worst-performing core pair (cores 1-5) were measured at two different temperatures (22 °C and 65 °C). The resulting power penalty was primarily caused by the temperature-induced clock phase shift. The clock phase was initially calibrated at 22 °C and the CDR was turned off during the BER measurements. As shown in Fig. 8, at 22 °C where the optimum clock phase was used, the receiver sensitivity at a BER of  $10^{-9}$  was -16.5 dBm. Increasing the temperature to 65 °C led to a 5.2 ps clock phase offset as indicated in the inset. Even with a 43 °C temperature increase, the power penalty was only 0.8 dB, and became error-free at > -15 dBm power. This confirms the resilience of MCF-based clock-synchronized interconnects.

#### IV. DISCUSSION

Our results show that MCF-based clock-synchronized transmission is able to tolerate more than 40 °C temperature variations, in excess of the recommended data centre air temperature guidelines [4]. Compared to the previous study using two SMF-28 of the same length, the low TCS of MCF allows for an order of magnitude higher tolerance to temperature variation [9]. Although the current experimental results are measured for 25.6 Gb/s OOK signals, they can be used to estimate the performance of high baud rate data

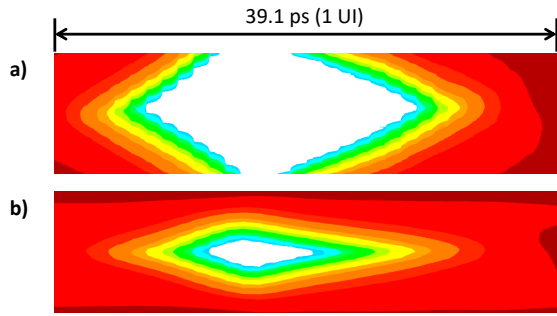


Fig. 6. Eye diagrams of received data signals at received optical powers of a) -10.5 dBm and b) -16.5 dBm, at the same temperature (22 °C).

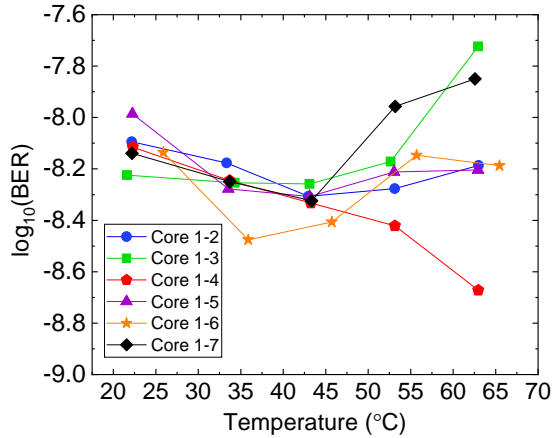


Fig. 7. Comparison of different MCF core pair performance against temperature at -16.5 dBm received power.

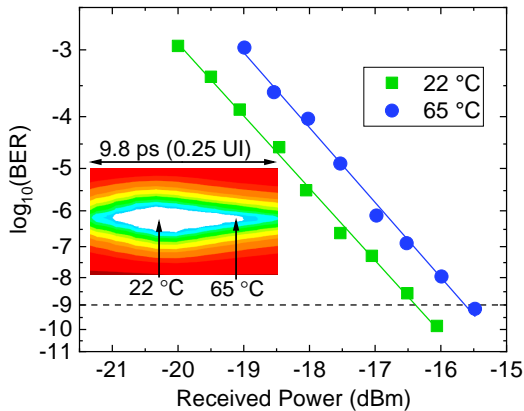


Fig. 8. Comparison of the performance for MCF core pair 1-5 against received signal power at 22 °C and 65 °C, with the inset eye diagram at -16.5 dBm received power indicating the clock sampling point at both temperatures.

transmission because the change of fiber temperature has negligible impact on signal qualities, as discussed in section III. Using the worst-case TCS value of 40 fs/km/°C from section II, assuming the same signal quality with an error-free eye width of up to 48% of a symbol period (from Fig. 6, 19 ps out of 39.1 ps), we can expect to see a temperature tolerance of 120 and 60 °C for 2-km MCF with 50 Gb/s and 100 Gb/s signals, respectively, both meeting the 40 °C temperature tolerance requirement [4]. In practice, the high

baud rate signals typically have worse signal qualities due to limited transceiver bandwidth and equalizers are commonly used to enhance the transmission performance [17]. Further study will be needed to understand the performance of clock-synchronized transmission using high baud rate signaling and advanced formats such as 4-level pulse amplitude modulation (PAM4). However, the results in this study show a potential route for low power consumption, low cost, CDR-free data communication using MCFs.

That noted, the proof-of-concept experiment shown in this paper aims at investigating the possibility of transmitting clock and data through different cores in an MCF. It is possible to transmit wavelength division multiplexed (WDM) signals in all the cores and to use one of the wavelengths to transmit the clock. This allows for sharing the same clock for all WDM channels transmitted through the same MCF, potentially reducing the number of CDR modules significantly, resulting in reduced power consumption and cost. This clock sharing scheme would not be possible if separate fibers are used.

An additional benefit of clock sharing is that it removes the need to transmit idle frames when no data is being sent through a link, which are normally required to keep receiver CDR modules locked. Data center links are typically heavily underutilised, with 99% of links only transmitting data 10% of the time [18]. The use of clock sharing could enable significant link power consumption improvements by allowing transmitters to turn off during idle periods since idle frames would not be required, without incurring long resynchronization time that occurs in standards such as Energy Efficient Ethernet [19].

Although the target application in this paper is intra-data center interconnection, the MCF-based clock-synchronized transmission can be used for many other applications. For example, in time-domain multiplexed passive optical networks (TDM-PON), clock synchronized transmission allows for a reduction of overhead that improves system efficiency. In radio-over-fiber (RoF) systems, multiple antennas can be synchronized with the same clock delivered through a fiber core. The large temperature tolerance demonstrated in this paper makes MCF-based clock-synchronized transmission promising for many field networking environments.

One of the main limitations of temperature-insensitive MCF for transmission systems is the requirement for co-propagating transmission of signals. Transmitting signals in the same direction through the fiber leads to strong correlation between core paths, resulting in a net cancellation of the TCDs between cores and therefore a TCS orders of magnitude lower than the core TCDs. However, in the case of counter-propagating transmission, the core TCDs will not cancel, resulting in similar values of the TCS and TCD. For this reason, the network architecture must be carefully considered if low thermal phase drift is required. However, it may still be beneficial to use MCF in bidirectional clock synchronized transmission systems, as the CDR can be removed in the direction where clock and data co-propagate, potentially halving the overall CDR required.

## V. CONCLUSION

We demonstrate, for the first time, optical clock-synchronized transmission without active clock phase tracking using multi-core fiber, showing zero bit errors across a 43 °C temperature range. This is enabled by the low thermal coefficient of skew of the multi-core fiber, below 40 fs/km/°C, measured using a delay interferometer. These results pave the way for potential CDR-free communication systems using optical clock synchronization methods, promising potentially significant reduced power consumption and cost.

## ACKNOWLEDGEMENTS

The authors would like to thank Microsoft for providing the FPGAs. The MCF fan-out was fabricated by Optoscribe.

## REFERENCES

- [1] H. Ballani, P. Costa, I. Haller, K. Jozwik, K. Shi, B. Thomsen, and H. Williams, "Bridging the last mile for optical switching in data centers," in *2018 Opt. Fiber Comm. Conf. (OFC)*, March 2018, pp. 1–3.
- [2] K. Clark, H. Ballani, P. Bayvel, D. Cletheroe, T. Gerard, I. Haller, K. Jozwik, K. Shi, B. Thomsen, P. Watts, H. Williams, G. Zervas, P. Costa, and Z. Liu, "Sub-nanosecond clock and data recovery in an optically-switched data centre network," in *2018 European Conference on Optical Communication (ECOC)*, Sep. 2018, pp. 1–3.
- [3] R. Slavik, G. Marra, E. N. Fokoua, N. Baddela, N. V. Wheeler, M. Petrovich, F. Poletti, and D. J. Richardson, "Ultralow thermal sensitivity of phase and propagation delay in hollow core optical fibres," *Scientific Reports*, vol. 5, no. 1, p. 15447, 2015. [Online]. Available: <https://doi.org/10.1038/srep15447>
- [4] ASHRAE TC9.9, "Data Centre Power Equipment Thermal Guidelines and Best Practices," 2016.
- [5] K. Clark, Y. Chen, E. Fokoua, T. Bradley, F. Poletti, D. Richardson, P. Bayvel, R. Slavik, and Z. Liu, "Low thermal sensitivity hollow core fibre for optically-switched data centre applications," in *2019 European Conference on Optical Communication (ECOC)*, Sep. 2019, pp. 1–3.
- [6] A. Cevrero, I. Ozkaya, T. Morf, T. Toifl, M. Seifried, F. Ellinger, M. Khafaji, J. Pliva, R. Henker, N. Ledentsov, J. Kropp, V. Shchukin, M. Zoldak, L. Halmo, I. Eddie, and J. Turkiewicz, "4×40 gb/s 2 pj/bit optical rx with 8ns power-on and cdr-lock time in 14nm cmos," in *2018 Optical Fiber Communications Conference and Exposition (OFC)*, March 2018, pp. 1–3.
- [7] A. Larsson, P. Westbergh, J. S. Gustavsson, E. Haglund, and E. P. Haglund, "High-speed VCSELs and VCSEL arrays for single- and multi-core fiber interconnects," in *Vertical-Cavity Surface-Emitting Lasers XIX*, C. Lei and K. D. Choquette, Eds., vol. 9381, International Society for Optics and Photonics. SPIE, 2015, pp. 103 – 113. [Online]. Available: <https://doi.org/10.1117/12.2082614>
- [8] T. Hayashi, A. Mekis, T. Nakanishi, M. Peterson, S. Sahni, P. Sun, S. Freyling, G. Armijo, C. Sohn, D. Foltz, T. Pinguet, M. Mack, Y. Kaneuchi, O. Shimakawa, T. Morishima, T. Sasaki, and P. De Dobbelaere, "End-to-end multi-core fibre transmission link enabled by silicon photonics transceiver with grating coupler array," in *2017 European Conference on Optical Communication (ECOC)*, Sep. 2017, pp. 1–3.
- [9] B. J. Puttnam, R. S. Luís, G. Rademacher, A. Alfredsson, W. Klaus, J. Sakaguchi, Y. Awaji, E. Agrell, and N. Wada, "Characteristics of homogeneous multi-core fibers for sdm transmission," *APL Photonics*, vol. 4, no. 2, p. 022804, 2019. [Online]. Available: <https://doi.org/10.1063/1.5048537>
- [10] B. J. Puttnam, G. Rademacher, R. S. Luís, J. Sakaguchi, Y. Awaji, and N. Wada, "Inter-core skew measurements in temperature controlled multi-core fiber," in *2018 Optical Fiber Communications Conference and Exposition (OFC)*, March 2018, pp. 1–3.
- [11] R. S. Luís, B. J. Puttnam, J. Delgado Mendinueta, W. Klaus, Y. Awaji, and N. Wada, "Comparing inter-core skew fluctuations in multi-core and single-core fibers," in *2015 Conference on Lasers and Electro-Optics (CLEO)*, May 2015, pp. 1–2.
- [12] A. Hartog, A. Conduit, and D. Payne, "Variation of pulse delay with stress and temperature in jacketed and unjacketed optical fibres," *Optical and Quantum Electronics*, vol. 11, no. 3, pp. 265–273, 1979.
- [13] G. Agrawal, *Fiber-Optic Communication Systems*, ser. Wiley Series in Microwave and Optical Engineering.
- [14] W. Hatton and M. Nishimura, "Temperature dependence of chromatic dispersion in single mode fibers," *Journal of Lightwave Technology*, vol. 4, no. 10, pp. 1552–1555, October 1986.
- [15] H. Yuan, A. Saljoghei, T. Hayashi, T. Nakanishi, E. Sillekens, L. Galdino, P. Bayvel, Z. Liu, and G. Zervas, "Experimental investigation of static and dynamic crosstalk in trench-assisted multi-core fiber," in *2019 Optical Fiber Communications Conference and Exhibition (OFC)*, March 2019, pp. 1–3.
- [16] "802.3bm-2015 - IEEE Standard for Ethernet - Amendment 3: Physical Layer Specifications and Management Parameters for 40 Gb/s and 100 Gb/s Operation over Fiber Optic Cables," *802.3bm-2015 - IEEE Standard for Ethernet Amendment 3: Physical Layer Specifications and Management Parameters for 40 Gb/s and 100 Gb/s Operation over Fiber Optic Cables*, pp. 1–172, March 2015.
- [17] E. P. da Silva and D. Zibar, "Widely linear equalization for IQ imbalance and skew compensation in optical coherent receivers," *Journal of Lightwave Technology*, vol. 34, no. 15, pp. 3577–3586, Aug 2016.
- [18] A. Roy, H. Zeng, J. Bagga, G. Porter, and A. C. Snoeren, "Inside the social network's (datacenter) network," in *Proceedings of the 2015 ACM Conference on Special Interest Group on Data Communication*, ser. SIGCOMM '15. New York, NY, USA: Association for Computing Machinery, 2015, p. 123–137. [Online]. Available: <https://doi.org/10.1145/2785956.2787472>
- [19] "Ieee standard for information technology– local and metropolitan area networks– specific requirements– part 3: Csma/cd access method and physical layer specifications amendment 5: Media access control parameters, physical layers, and management parameters for energy-efficient ethernet," *IEEE Std 802.3az-2010 (Amendment to IEEE Std 802.3-2008)*, pp. 1–302, Oct 2010.